

Structure of Hydrated Tungsten Peroxides [WO₂(O₂)H₂O]·nH₂O

Brigitte Pecquenard,^{†,‡} Socorro Castro-Garcia,[†] Jacques Livage,^{*,†}
Peter Y. Zavalij,[‡] M. Stanley Whittingham,[‡] and René Thouvenot[§]

*Chimie de la Matière Condensée, University Paris VI, 4 place Jussieu, 75252 Paris, France;
Chemistry Department and Materials Research Center, State University of New York at
Binghamton, Binghamton, New York 13902-6000; and Chimie des Métaux de Transition,
University Paris VI, 4 place Jussieu, 75252 Paris, France*

Received January 26, 1998

Hydrated tungsten peroxides have been synthesized via the reaction of tungstic acid, H₂WO₄, with aqueous solutions of hydrogen peroxide. Two crystalline phases with the formula [WO₂(O₂)H₂O]·nH₂O were obtained. X-ray powder diffraction data show that these two phases crystallize with monoclinic symmetry. Their structures were solved by using direct methods, and then full profile Rietveld refinements were carried out. As in other peroxo compounds, the coordination polyhedron around W^{VI} can be described by a [WO₆] distorted octahedron in which one corner is replaced by a peroxo ligand (O₂). Both structures are made of zigzag double chains built up of edge-sharing octahedra along the *b*-axis. Coordinated water molecules join the chains to make the layers. In the case of *n* ≠ 0, additional water molecules link the layers together through hydrogen bonds.

Introduction

Peroxo tungstic acids are known to exhibit interesting properties. They can be used as electrochromic coatings,¹ proton conductors,^{2,3} photoresists,⁴ or optical waveguides.⁵

Peroxo tungstic acids have been synthesized by Kudo et al. via the dissolution of tungsten metal or tungsten carbide in H₂O₂.^{6,7} They are soluble in polar solvents such as water or alcohol and can be easily spin- or dip-coated on various substrates. A yellow amorphous solid is obtained when the solution is rapidly evaporated in a stream of air at room temperature. Several empirical formulas, WO₃·xH₂O₂·yH₂O (*x* = 0.69 and *y* = 2.25 or *x* = 0.58 and *y* = 1.66) have been suggested in the literature.^{2,8} This water-soluble amorphous solid decomposes upon heating, giving an insoluble material. Therefore, thin films have to be heated around 120 °C before use as electrochromic layers.¹

A crystalline peroxopolytungstic acid, WO₃·H₂O₂·H₂O, has also been synthesized by Kudo et al.⁹ It turned into another crystalline powder, WO₃·0.94H₂O₂·0.14H₂O, when heated to about 120 °C.¹ These materials exhibit interesting properties as inorganic photoresists. They are sensitive toward ultraviolet light and become soluble in water or methanol after UV irradiation.³

According to Kudo, amorphous peroxopolytungstic acid is supposed to be made of peroxo polytungstate anions linked together by hydrogen bonding. Radial distribution functions suggest that these anions are [W₁₂O₃₈(O₂)₆]¹⁶⁻ in which a six-membered ring of corner-sharing [WO₅(O₂)] and [WO₆] polyhedra is sandwiched by two [W₃O₁₀] units.⁸⁻¹⁰ The structure of crystalline compounds has not yet been fully resolved, either. According to previous work, they are proposed to have layered structures with basal spacings of 8.98 and 6.84 Å, respectively. The 2.15 Å difference should be due to water molecules inserted between the layers.³

This paper presents a detailed structural study of two crystalline tungsten peroxide hydrates formed from aqueous solutions of W^{VI} in H₂O₂.

Experimental Section

¹⁸³W NMR of Peroxopolytungstic Acid Solutions. Peroxopolytungstic acid solutions were prepared via the dissolution of tungstic acid in hydrogen peroxide. A commercial H₂WO₄ powder (12.5 g) was mixed with 100 mL of an aqueous solution of H₂O₂ (30%, pH 3.9), free of H₃PO₄, and heated with magnetic stirring at 60 °C for few hours until complete dissolution. A clear colorless acid solution was formed (pH 1.7).

* Corresponding author. Phone: (33) 1 44 27 33 65. Fax: (33) 1 44 27 47 69. E-mail: livage@ccr.jussieu.fr.

[†] Chimie de la Matière Condensée, University Paris VI.

[‡] State University of New York at Binghamton.

[§] Chimie des Métaux de Transition, University Paris VI.

(1) Yamanaka, K.; Okamoto, H.; Kidou, H.; Kudo, T. *Jpn. J. Appl. Phys.* **1986**, *25*, 1420.

(2) Okamoto, H.; Yamanaka, K.; Kudo, T. *Mater. Res. Bull.* **1986**, *21*, 551.

(3) Hibino, M.; Nakajima, H.; Kudo, T.; Mizumo, N. *Solid State Ionics* **1997**, *100*, 211.

(4) Okamoto, H.; Ishikawa, A.; Kudo, T. *J. Electrochem. Soc.* **1989**, *136*, 2646.

(5) Itoh, K.; Okamoto, T.; Wakita, S.; Niikura, H.; Murabayashi, M. *Appl. Organomet. Chem.* **1991**, *5*, 295.

(6) Kudo, T. *Nature* **1984**, *312*, 537.

(7) Kudo, T.; Okamoto, H.; Matsumoto, K.; Sasaki, Y. *Inorg. Chim. Acta* **1986**, *111*, L27.

(8) Okamoto, H.; Ishikawa, A.; Kudo, T. *Bull. Chem. Soc. Jpn.* **1989**, *62*, 2723.

(9) Kudo, T.; Oi, J.; Kishimoto, A.; Hiratani, M. *Mater. Res. Bull.* **1991**, *26*, 779.

(10) Nanba, T.; Takano, S.; Yasui, I.; Kudo, T. *J. Solid State Chem.* **1991**, *90*, 47.

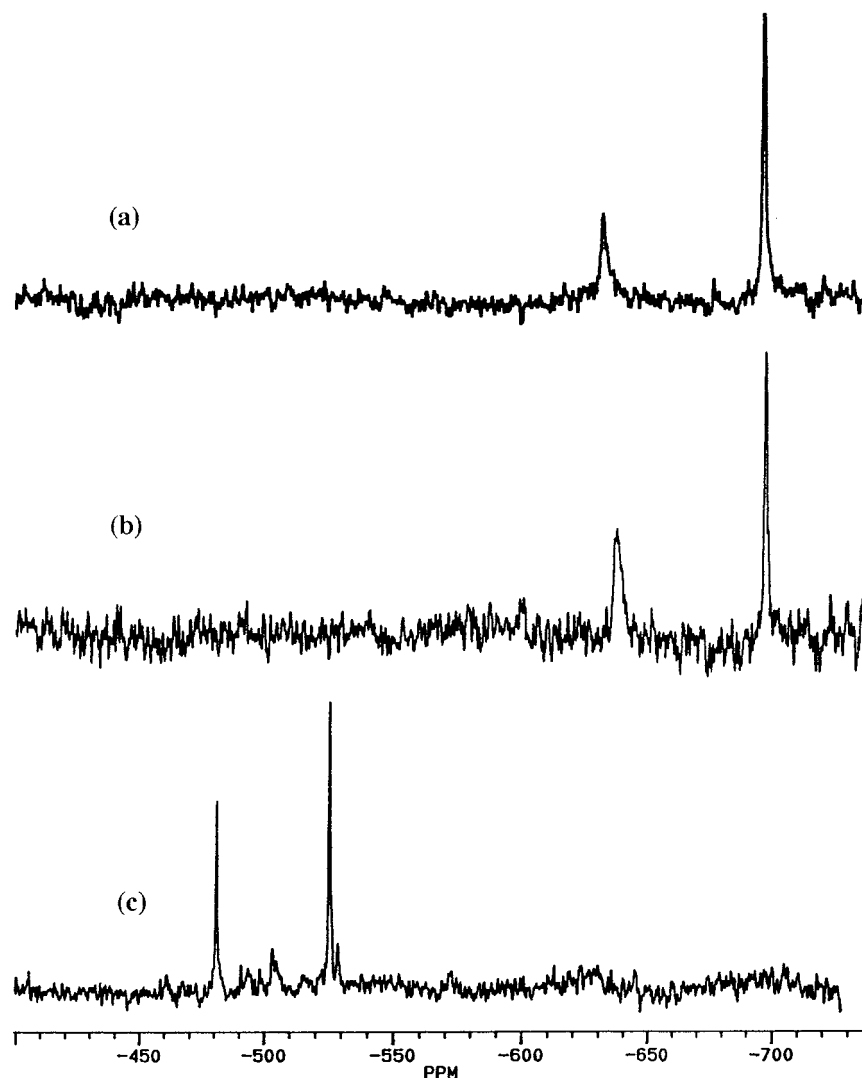


Figure 1. ^{183}W NMR spectra of aqueous solutions of H_2WO_4 in H_2O_2 . (a) Fresh solution with an excess of H_2O_2 , (b) solution after dipping a Pt net, and (c) solution refluxed at $90^\circ C$ for 10 h.

^{183}W NMR experiments were performed on these solutions with a Bruker AC 300 spectrometer at 12.5 MHz, equipped with a tunable VSP probe head. Chemical shifts are given with respect to Na_2WO_4 aqueous solution (2 M) and were determined via the substitution method using a saturated $H_4SiW_{12}O_{40}$ solution in D_2O as a secondary standard ($\delta -103.8$ ppm). As the sensitivity of the ^{183}W nucleus is very weak (natural abundance 14.4%; $\gamma = 1.12 \times 10^7 \text{ rad T}^{-1} \text{ s}^{-1}$), NMR spectra had to be accumulated for a long time (10–20 h, >20 000 scans) to get a reasonable signal/noise ratio.

Results and Discussion

The ^{183}W NMR spectrum of a peroxotungstic solution ($[W] = 0.5 \text{ M}$) exhibits two peaks in a $\sim 2/1$ ratio (Figure 1a). The first one, at $\delta -696.5$ ppm, could be assigned to the dimeric peroxy anion $[W_2O_3(O_2)_4(H_2O)_2]^{2-}$.¹¹ The second one, at $\delta -631.2$ ppm ($\Delta\nu_{1/2} > 20 \text{ Hz}$), was already observed in phosphato peroxotungstic aqueous solutions ($\delta -628$ ppm).¹² It was recently assigned by Kudo et al. to the monomeric dioxodiperoxy anion,

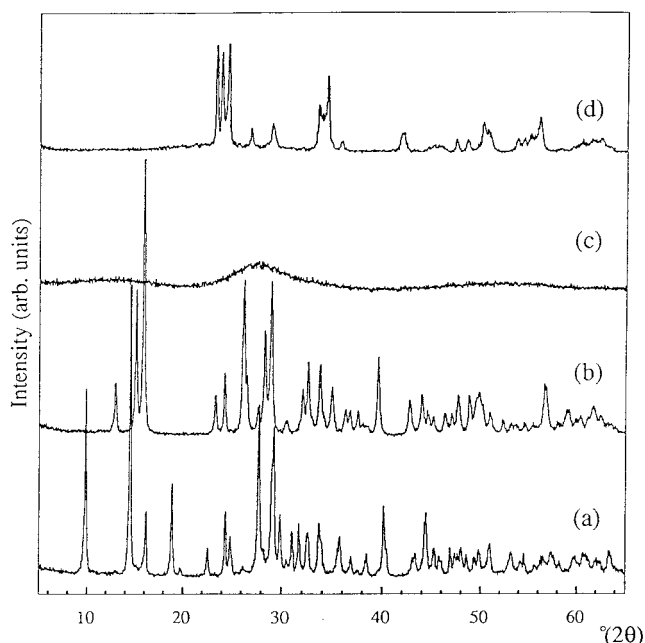


Figure 2. X-ray diffraction patterns of peroxopolytungstate powders heated at different temperatures. (a) Room temperature, (b) $120^\circ C$, (c) $230^\circ C$, and (d) $400^\circ C$.

(11) Campbell, N. J.; Dengel, A. C.; Edwards, C. J.; Griffith, W. P. *J. Chem. Soc., Dalton Trans.* **1989**, 1203.

(12) Aubry, C.; Chottard, G.; Platzner, N.; Brégeault, J. M.; Thouvenot, R.; Chauveau, F.; Huet, C.; Ledon, H. *Inorg. Chem.* **1991**, *30*, 4409.

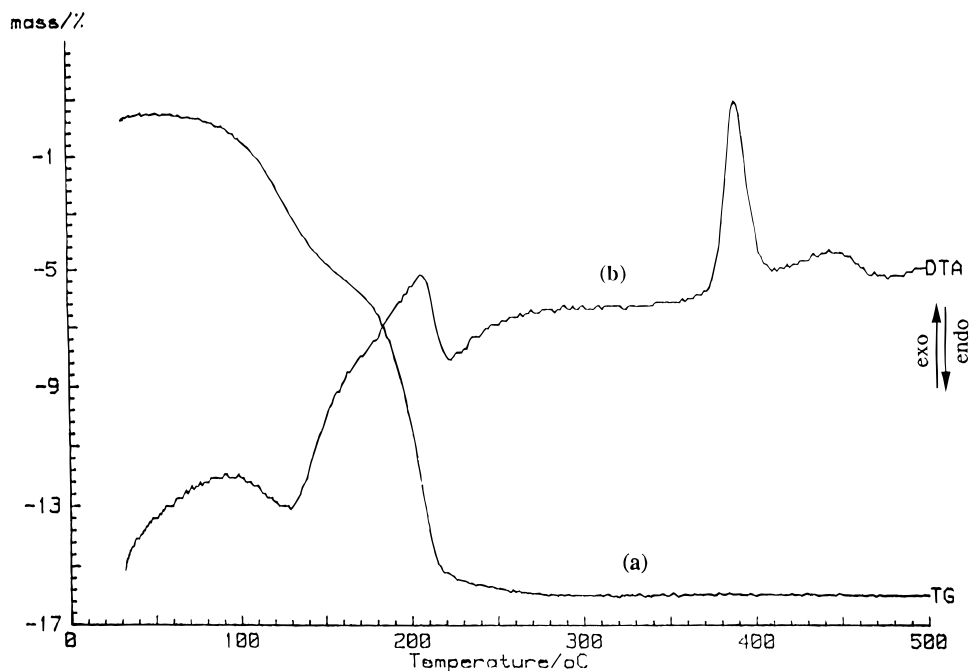


Figure 3. Thermal analysis of a $[\text{WO}_2(\text{O}_2)\text{H}_2\text{O}] \cdot n\text{H}_2\text{O}$ powder (phase W_1). (a) Thermogravimetric analysis and (b) differential thermal analysis (O_2 flow, $5^\circ\text{C}/\text{min}$).

$[\text{WO}_2(\text{O}_2)_2]^{2-}$, on the basis of a correlation between the chemical shift and the ratio of the number of peroxo groups to that of W.¹³ It has to be pointed out that both peaks are very broad compared to those usually observed for oxo tungstate and phosphato oxoperoxo tungstates ($\Delta\nu_{1/2} < 5$ Hz).

Except for a further broadening, especially for the -631 ppm peak, the ^{183}W NMR spectrum does not change significantly when the solution is aged at room temperature or when H_2O_2 in excess is removed by dipping a platinum net in the solution (Figure 1b). Both peaks remain visible even after several weeks under ambient conditions. Refluxing the solution at 90°C for 10 h leads to a yellow solution that exhibits a completely different ^{183}W NMR spectrum (Figure 1c). Two main peaks are then observed at higher frequency, in the less shielding part of the spectrum ($\delta -525.5$ and -480.9 ppm). Compared to the previous spectra, both are remarkably narrow ($\Delta\nu_{1/2} < 5$ Hz). Another weak line is also observed at $\delta -180$ ppm. According to the literature, the substitution of oxo ligands for peroxo groups in the coordination sphere of W^{VI} induces deshielding of the tungsten nucleus.¹³ Both peaks around -500 ppm could be assigned to species containing only one peroxo group per tungsten. The peak at -180 ppm should be assigned to oxotungstates that usually give ^{183}W NMR signals between -100 and -200 ppm.¹⁴ The relatively poor signal/noise ratio does not allow any accurate measurements of the intensity ratio of these three lines. It is therefore not possible to tell whether they correspond to different species such as $[\text{WO}_3(\text{O}_2)]^{2-}$ and $[\text{W}_2\text{O}_5(\text{O}_2)_2(\text{H}_2\text{O})_2]^{2-}$ or to a single, more or less condensed oxoperoxo polytungstate.

Crystalline Peroxopolytungstic Acids. According to the literature, the rapid evaporation in a stream of

air of a solution of peroxopolytungstic acid leads to the formation of a yellow amorphous solid, $\text{WO}_3 \cdot x\text{H}_2\text{O}_2 \cdot y\text{H}_2\text{O}$, with $0.05 \leq x \leq 1$ and $3 \leq y \leq 4$.¹ However, a white crystalline powder is obtained when the aqueous solution is evaporated slowly at room temperature (Figure 2a). Let us call this crystalline phase " W_1 ".

The thermal analyses of this crystalline powder were performed under an oxygen flow at a heating rate of $5^\circ\text{C}/\text{min}$. They show two weight losses associated with two endothermic peaks at about 120 and 200°C (Figure 3). The first weight loss ($\sim 6\%$) depends on the drying procedure and should correspond to the departure of weakly bonded water molecules ($\text{H}_2\text{O}/\text{W} \approx 1-2$). The second peak always corresponds to a weight loss of 12% . It should be due to the departure of more strongly bonded coordinated water molecules ($\text{H}_2\text{O}/\text{W} = 1$) and the decomposition of peroxo groups. X-ray diffraction experiments performed on the powder heated at different temperatures show that another crystalline phase, " W_2 ", is formed at 120°C (Figure 2b). This crystalline compound decomposes upon further heating above 200°C , giving an amorphous powder (Figure 2c) that then crystallizes into monoclinic WO_3 as shown by its X-ray diffraction diagram (Figure 2d). The exothermic peak seen on DTA curves at 390°C should then correspond to the crystallization of amorphous tungsten oxide (Figure 3b).

Infrared absorption spectra were recorded on powders dispersed in KBr pellets using a Fourier transform Nicolet spectrometer working between 500 and 4000 cm^{-1} . The infrared absorption spectra of the two crystalline powders are very similar in the low-wavenumber region (Figure 4). As is usually observed for polyoxometalates, the more hydrated form (W_1) exhibits broader vibrational bands. According to the literature, the four intense bands can be assigned respectively to $\nu_s \text{W}=\text{O}$ (968 cm^{-1}), $\nu \text{O}-\text{O}$ (903 cm^{-1}), $\nu_{\text{as}} \text{W}-\text{O}-\text{W}$ (650 cm^{-1}), and $\nu_{\text{as}} \text{W}(\text{O}_2)$ (540 cm^{-1}).⁹⁻¹² However, these

(13) Nakajima, H.; Kudo, T.; Mizumo, N. *Chem. Lett.* **1997**, 693.

(14) Pope, M. T. *Heteropoly and Isopoly Oxometalates*, Springer-Verlag: Berlin, 1983.

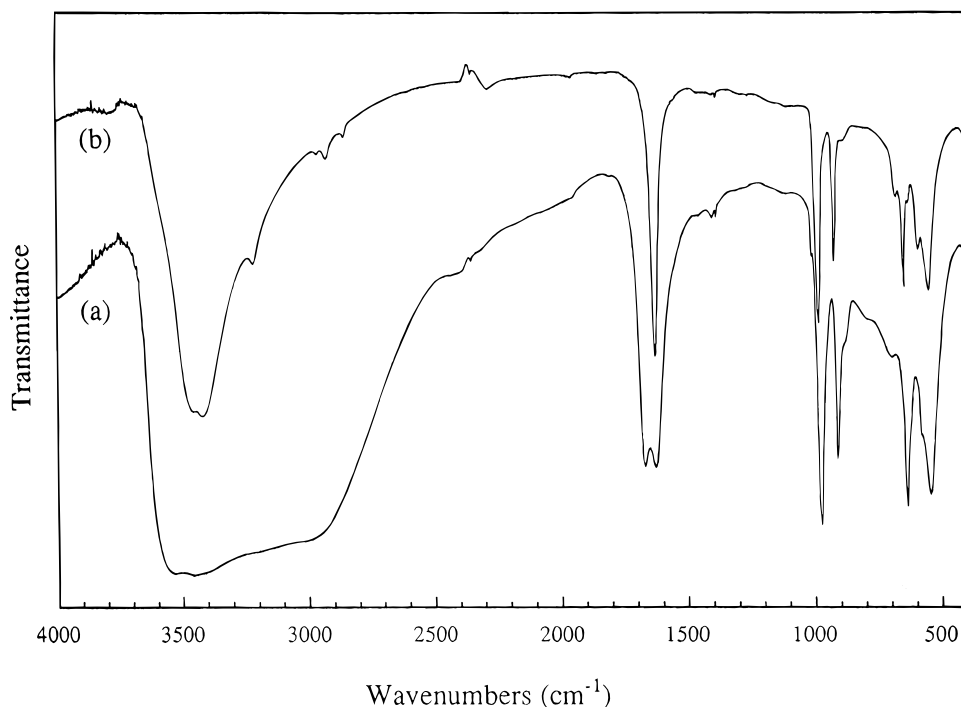


Figure 4. Infrared absorption spectra of crystalline tungsten peroxide hydrates. (a) $[\text{WO}_2(\text{O}_2)\text{H}_2\text{O}] \cdot n\text{H}_2\text{O}$ (phase W_1) and (b) $[\text{WO}_2(\text{O}_2)\text{H}_2\text{O}]$ (phase W_2).

spectra differ significantly at higher frequency in the region where the vibrations of water molecules are expected to occur. The less hydrated W_2 phase (Figure 4b) exhibits a sharp band at 1620 cm^{-1} (OH bending) and two bands at 3405 cm^{-1} ($\nu_s \text{ H}_2\text{O}$) and 3450 cm^{-1} ($\nu_{as} \text{ H}_2\text{O}$). This suggests the presence of a single kind of loosely hydrogen bonded water molecule.¹⁵

The infrared spectrum of the more hydrated W_1 phase (Figure 4a) is obviously more complex, in both bending and stretching regions. This suggests the presence of different kinds of water molecules. The broad absorption band around 2900 cm^{-1} ($\Delta\nu \approx 300\text{ cm}^{-1}$) could correspond to the stretching vibration of an OH group involved in an intermediate hydrogen bond ($d_{\text{O}-\text{O}} \approx 2.6\text{--}2.7\text{ \AA}$). It would be associated with the bending band observed at 1700 cm^{-1} .

Structure Determination by Powder X-ray Diffraction. X-ray powder diffraction was performed using Cu $K\alpha$ radiation ($\lambda = 1.5418\text{ \AA}$) on a Scintag XDS2000 $\theta\text{--}\theta$ diffractometer. The data were collected from $8^\circ 2\theta$ to $72^\circ 2\theta$ and from $10^\circ 2\theta$ to $69.5^\circ 2\theta$, respectively, for W_1 and W_2 with $0.03^\circ 2\theta$ steps and 15 s per step.

The general formulas of both phases were deduced from thermal analyses and X-ray diffraction measurements, which lead to $[\text{WO}_2(\text{O}_2)\text{H}_2\text{O}] \cdot n\text{H}_2\text{O}$ for phase W_1 , with $1 \leq n \leq 2$ depending on drying conditions, and $[\text{WO}_2(\text{O}_2)\text{H}_2\text{O}]$ for phase W_2 . The powder diffraction patterns of the two phases were indexed in a monoclinic system using the Ito method from the CSD software.¹⁶ Space group $C2/m$ was chosen for the W_1 phase, and $P2_1/c$ was clearly assigned for the W_2 phase from the absence of the $0k0$ and $h0l$ reflections. The cell param-

Table 1. Crystallographic Data for $[\text{WO}_2(\text{O}_2)\text{H}_2\text{O}] \cdot n\text{H}_2\text{O}$ (Phase W_1) and $[\text{WO}_2(\text{O}_2)\text{H}_2\text{O}]$ (Phase W_2)

compd	$[\text{WO}_2(\text{O}_2)\text{H}_2\text{O}] \cdot n\text{H}_2\text{O}$	$[\text{WO}_2(\text{O}_2)\text{H}_2\text{O}]$
space group	$C2/m$	$P2_1/c$
a (\AA)	12.4110(7)	12.0710(8)
b (\AA)	3.8717(3)	3.8643(2)
c (\AA)	10.1405(6)	12.6568(9)
β (deg)	117.553(3)	145.470(3)
cell vol (\AA^3)	432.00(5)	334.65(8)
calcd density (g/cm^3)	4.547	5.276
formula wt (g/mol)	295.8	263.8
absorption coeff (cm^{-1})	506.1	645.9
radiation and wavelength	Cu $K\alpha$, 1.54178 \AA	Cu $K\alpha$, 1.54178 \AA
diffractometer	Scintag XDS2000	Scintag XDS2000
indexing method	Ito	Ito
structure determination	direct methods	direct methods
software	CSD	CSD
final refinement	GSAS	GSAS
mode of refinement	full profile	full profile
max 2θ	72	69.5
no. of refined parameters	31	33
no. of reflections	124	143
$R(F^2)$	0.090	0.045
$R(p)$	0.061	0.053
$Rw(p)$	0.082	0.069
min/max Δ/σ	-0.10/0.07	-0.12/0.01
min/max $\Delta\rho$	-0.95/1.11	-0.75/0.83

eters are: $a = 12.4110(7)\text{ \AA}$, $b = 3.8717(3)\text{ \AA}$, $c = 10.1405(6)\text{ \AA}$ and $\beta = 117.553(3)^\circ$ for the first phase and $a = 12.0710(8)\text{ \AA}$, $b = 3.8643(2)\text{ \AA}$, $c = 12.6568(9)\text{ \AA}$ and $\beta = 145.470(3)^\circ$ for the second one. Integrated intensities of 117 and 67 peaks, respectively, for the first and second phases were used in direct methods to solve the structures. First, W and some O atoms were located from the E map, and then the remaining O atoms (including those belonging to water molecules) were found from difference Fourier maps. The final refinement was achieved for both phases by using the GSAS

(15) Novak, A. *Struct. Bonding* **1974**, *18*, 177.

(16) Akselrud, L. G.; Zavalij, P. Y.; Grin, Y. N.; Pecharsky, V. K.; Baumgartner, B.; Wolfel, E. *Mater. Sci. Forum* **1993**, *133*, 335.

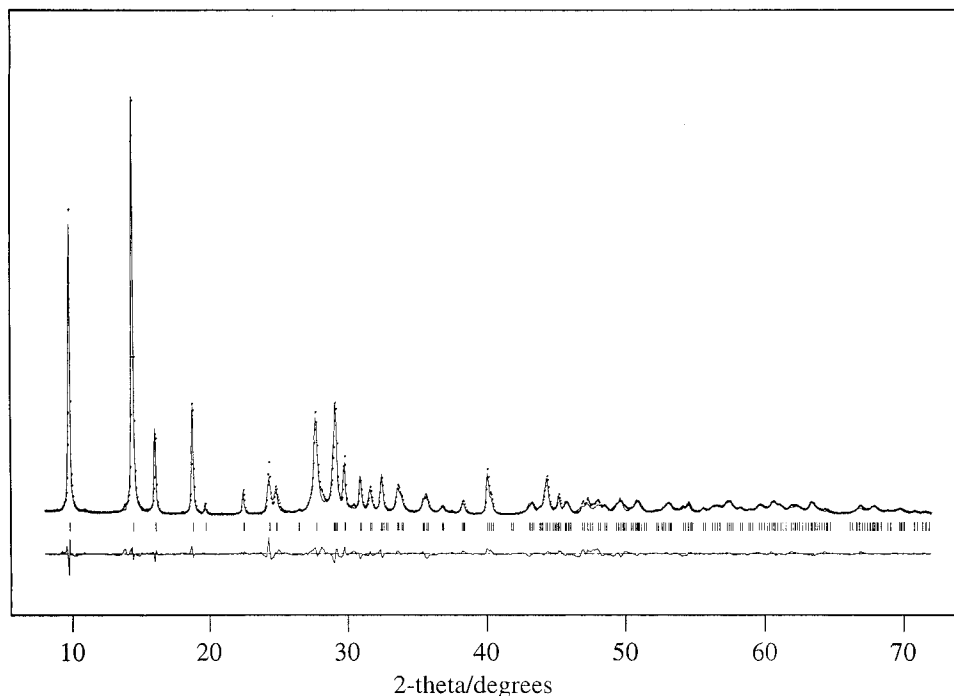


Figure 5. Calculated X-ray pattern resulting from a final Rietveld refinement (thin line), experimental data (dotted line), and a difference plot (on the bottom) for $[\text{WO}_2(\text{O}_2)\text{H}_2\text{O}] \cdot n\text{H}_2\text{O}$ (phase W_1).

Table 2. Atomic Coordinates and Thermal Parameters for $[\text{WO}_2(\text{O}_2)\text{H}_2\text{O}] \cdot n\text{H}_2\text{O}$ and $[\text{WO}_2(\text{O}_2)\text{H}_2\text{O}]$

atom	x/a	y/b	z/c	U_{iso}	multiple occupancy
[$\text{WO}_2(\text{O}_2)\text{H}_2\text{O}] \cdot n\text{H}_2\text{O}$					
W	0.8350(3)	0	0.1418(4)	0.038(2)	4
O1	0.974(2)	0	0.129(3)	0.019(2)	4
O2	0.292(2)	0	0.097(3)	0.019(2)	4
O3	0.883(1)	0.147(4)	0.343(2)	0.019(2)	8
O4	0.658(2)	0	0.162(3)	0.019(2)	4
H ₂ O	0.360(2)	0.177(4)	0.589(2)	0.05(2)	8 0.83(2)
[$\text{WO}_2(\text{O}_2)\text{H}_2\text{O}]$					
W	0.1831(4)	0.0670(6)	0.3629(4)	0.025(1)	4
O1	0.167(4)	0.079(6)	0.221(3)	0.04(4)	4
O2	0.129(4)	0.562(6)	0.336(3)	0.04(4)	4
O3	0.461(4)	0.256(6)	0.600(4)	0.04(4)	4
O4	0.432(4)	-0.106(7)	0.569(3)	0.04(4)	4
O5	0.204(2)	0.031(5)	0.565(2)	0.04(4)	4

program,¹⁷ and the results are collected in Table 1. The refinement gave $R(\text{profile}) = 0.061$ for the first phase and $R(\text{profile}) = 0.053$ for the second one. The atomic positions and interatomic distances are given in Tables 2 and 3, respectively. The powder X-ray diffraction patterns of the observed and calculated data after Rietveld refinement are shown in Figures 5 and 6, respectively.

In these structures, the coordination polyhedron around W can be described as a distorted octahedron $[\text{WO}_6]$ where one corner is replaced by a peroxy group. Three oxygens and the peroxy group lie on the equatorial plane, whereas apical positions are occupied by a water molecule and a double-bonded oxygen. These octahedra assembled together by sharing edges, forming double zigzag chains along the b -axis (Figure 7). The $\text{W}=\text{O}$ double bonds belonging to a pair of octahedra are

Table 3. W–O Interatomic Distances for $[\text{WO}_2(\text{O}_2)\text{H}_2\text{O}] \cdot n\text{H}_2\text{O}$ and $[\text{WO}_2(\text{O}_2)\text{H}_2\text{O}]$

[$\text{WO}_2(\text{O}_2)\text{H}_2\text{O}] \cdot n\text{H}_2\text{O}$		[$\text{WO}_2(\text{O}_2)\text{H}_2\text{O}]$	
bond	distance	bond	distance
$\text{W}=\text{O}1$	1.79(3)	$\text{W}=\text{O}1$	1.64(2)
$\text{W}\cdots\text{O}4$	2.30(3)	$\text{W}\cdots\text{O}5$	2.36(2)
$\text{W}-\text{O}2$	2.00(1)	$\text{W}-\text{O}2$	1.96(2)
$\text{W}-\text{O}2$	2.00(1)	$\text{W}-\text{O}2$	2.00(2)
$\text{W}-\text{O}2$	2.20(2)	$\text{W}-\text{O}2$	2.21(2)
$\text{W}-\text{O}3$	1.92(2)	$\text{W}-\text{O}3$	2.05(2)
$\text{W}-\text{O}3$	1.92(2)	$\text{W}-\text{O}4$	1.83(2)

turned in opposite directions. For the first structure, the cation–anion distances in the polyhedra vary from 1.79 Å, corresponding to double bond $\text{W}=\text{O}$, to 2.30 Å, with an average value of 2.02 Å. The structure of W_1 contains two types of water molecules (Figure 8). The coordination water joins chains in the layers through hydrogen bonds along the a -axis. The second type is a water of crystallization which is weakly bound and links layers together, also through hydrogen bonds, along the c -axis. This water is eliminated by a thermal treatment at 120 °C.

In the second phase, W_2 , the characteristic polyhedron is little more distorted, with cation–anion distances varying from 1.64 Å (corresponding to a double bond, $\text{W}=\text{O}$) to 2.36 Å, with an average value of 2.01 Å. In the structure of W_2 , the water of crystallization is removed and only the coordination water remains. The structure is very close to the previous one. The layers are also made by double zigzag chains linked together through hydrogen bonds, but they become closer (Figure 9). Like this, although the c -parameter is higher for this phase, the d spacing is decreased from 8.99 to 7.17 Å. Moreover, the distance between two W atoms along the layer is equal to 6.4 Å instead of 5.6 Å in the first structure.

(17) Larsen, C. A.; Von Dreele, R. B. *GSAS: General Structure Analysis System*; Los Alamos National Laboratory: Los Alamos, New Mexico.

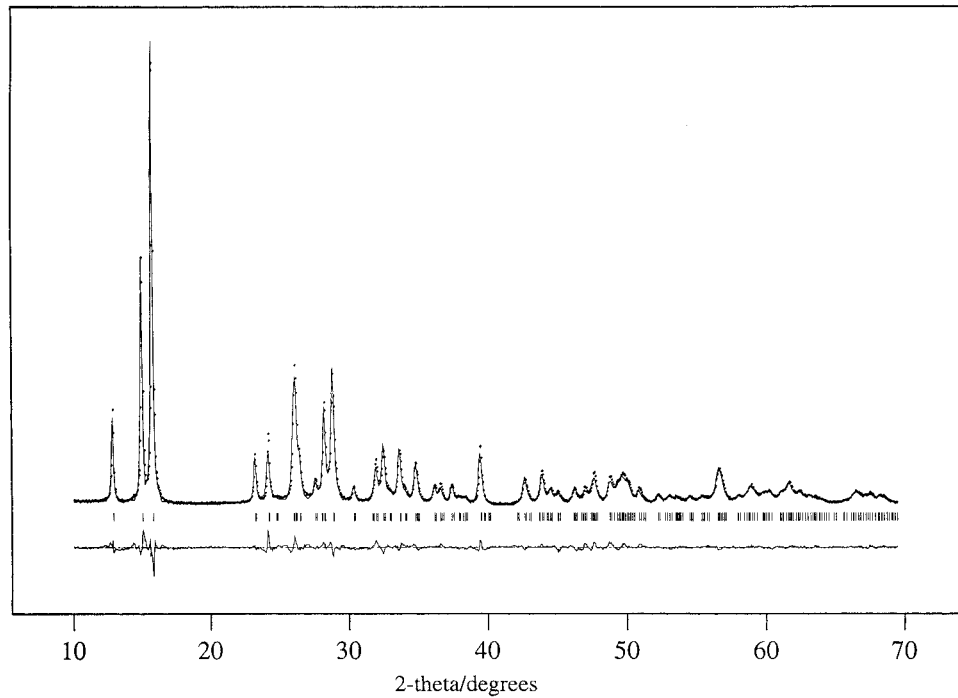


Figure 6. Calculated X-ray pattern resulting from a final Rietveld refinement (thin line), experimental data (dotted line), and a difference plot (on the bottom) for $[\text{WO}_2(\text{O}_2)\text{H}_2\text{O}]$ (phase W_2).

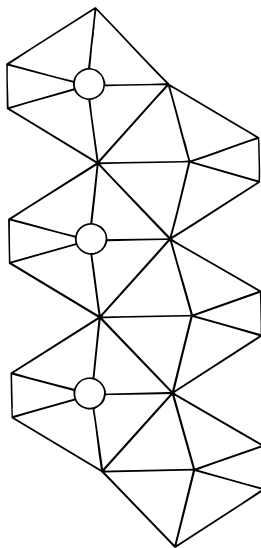


Figure 7. Representation along the b -axis of a double zigzag chain made of edges sharing distorted octahedra. Empty circles (O) correspond to tungsten atoms.

Conclusion

The slow drying of peroxopolytungstic acid solutions leads to the formation of a crystalline phase, W_1 , that upon thermal dehydration at 120°C transforms into another crystalline phase, W_2 . According to their powder X-ray diffraction patterns, these tungsten peroxide hydrates should correspond to the two crystalline $\text{WO}_3 \cdot x\text{H}_2\text{O}_2 \cdot y\text{H}_2\text{O}$ phases ($x = 1$ and $y = 1$ or $x = 0.94$ and $y = 0.14$) of unknown structure reported earlier by Kudo et al.^{9,10} However, our results do not agree with the chemical formula suggested by these authors.

The detailed analysis of the structure of both crystalline phases W_1 and W_2 leads to $[\text{WO}_2(\text{O}_2)(\text{H}_2\text{O})] \cdot n\text{H}_2\text{O}$

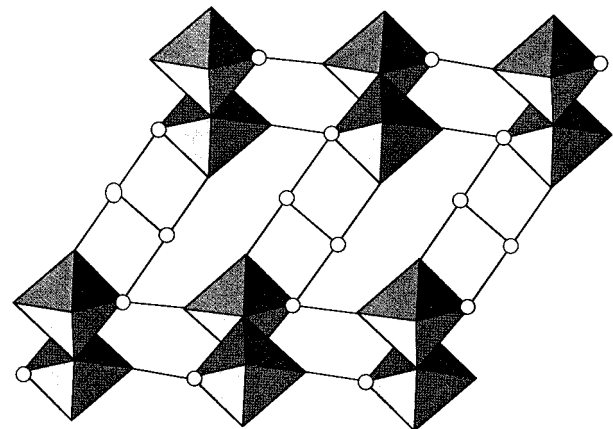


Figure 8. Structure of $[\text{WO}_2(\text{O}_2)\text{H}_2\text{O}] \cdot n\text{H}_2\text{O}$. The circles (O) correspond to water molecules.

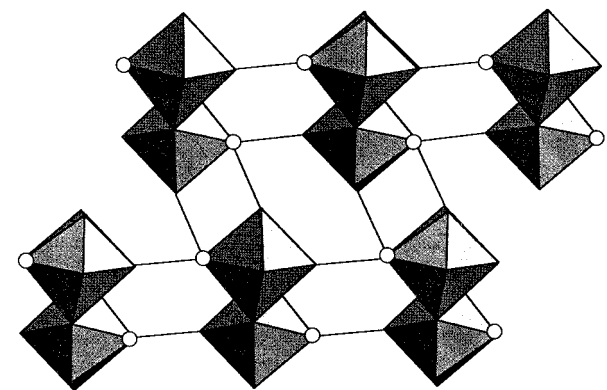
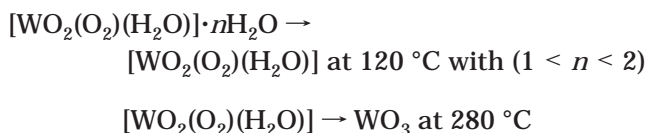


Figure 9. Structure of $[\text{WO}_2(\text{O}_2)\text{H}_2\text{O}]$. Only coordinated water molecules remain in the structure (circles, O).

for the room-temperature phase and $[\text{WO}_2(\text{O}_2)(\text{H}_2\text{O})]$ for the phase obtained upon heating at 120°C . The two successive weight losses observed by thermal analysis

should then correspond to the following transformations:



Peroxo complexes of W^{VI} have been shown to be formed in aqueous solutions of H_2O_2 .¹⁸ Peroxo tungstates are not stable at high pH ($\text{pH} > 9$), but the monomeric anion $[\text{W}(\text{O}_2)_4]^{2-}$ is formed in mildly alkaline solutions ($\text{pH} \approx 9$). Condensation occurs below pH 5 giving the dimeric tetraperoxotungstate anion $[\text{W}_2\text{O}_3(\text{O}_2)_4(\text{H}_2\text{O})_2]^{2-}$. Crystalline solids can be precipitated from these acid solutions by adding cations, giving, for instance, the potassium salt $\text{K}_2\text{W}_2\text{O}_{11} \cdot 4\text{H}_2\text{O}$. The crystal structure of this compound shows that tetraperoxoditungstate anions contain two tungsten atoms linked by a single nonlinear oxygen bridge. Each tungsten atom is surrounded by a pentagonal bipyramid $[\text{WO}_2(\text{O}_2)_2(\text{H}_2\text{O})]$. Peroxo groups are in the equatorial plane, while apical positions are occupied by a water molecule and a double-bonded oxygen.¹⁹ Monomeric diperoxo species such as $[\text{WO}(\text{O}_2)_2(\text{H}_2\text{O})_2]$ or $[\text{WO}(\text{O}_2)_2(\text{OH})(\text{H}_2\text{O})]^-$ should be formed in dilute acidic solutions, but the complexing behavior of peroxo ligands prevents condensation.

Peroxo complexes are known to be thermodynamically unstable and to decompose slowly, giving tungsten trioxide, WO_3 , and polytungstates $[\text{W}_{12}\text{O}_{39}]$.⁶⁻²⁰ We have shown that under mild conditions, the slow evaporation of a solution of peroxopolytungstic acid leads to the formation of a white crystalline powder

(18) Dickman, M. H.; Pope, M. T. *Chem. Rev.* **1994**, *94*, 569.

(19) Einstein, F. W. B.; Penfold, B. R. *Acta Crystallogr.* **1964**, *17*, 1127.

(20) Meulenkamp, E. A. *J. Electrochem. Soc.* **1997**, *144*, 1664.

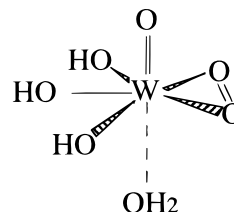


Figure 10. Suggested monoperoxo molecular precursor $[\text{WO}(\text{OH})_3(\text{O}_2)(\text{H}_2\text{O})]$.

$[\text{WO}_2(\text{O}_2)\text{H}_2\text{O}] \cdot n\text{H}_2\text{O}$. It may be suggested that such a solid could be formed via the condensation of monoperoxo precursors such as $[\text{WO}(\text{OH})_3(\text{O}_2)(\text{H}_2\text{O})]$ in which the O_2/W ratio is about 1 (Figure 10).²⁰ Condensation reactions would involve the three $\text{W}-\text{OH}$ groups in the equatorial plane leading to the formation of double chains of edge-sharing bipyramids linked by $\mu_3\text{-O}$ oxo bridges (Figure 7). The concentration of such a hypothetical precursor might be too small to detect by ^{183}W NMR.

Thermal treatment at 120°C and removal of water molecules gives a second crystalline phase, $[\text{WO}_2(\text{O}_2)\text{H}_2\text{O}]$. These two compounds have a monoclinic symmetry. Both structures can be described by double zigzag chains built up from edge-sharing octahedra along the b -axis. The chains are linked together through hydrogen bonds, forming layers. In both phases, W^{VI} is 7-fold coordinated with a pentagonal bipyramidal geometry based on $[\text{WO}_6]$ octahedra in which an oxygen is replaced by a chelating peroxo group, $[\text{O}_2]^{2-}$. Such a coordination is quite usual in peroxo complexes of W^{VI} .¹⁸

Acknowledgment. The work at Binghamton was partially supported by the National Science Foundation under grant DMR-9422667 and the ICDD under a grant in aid.

CM980045N